

Transport of Axl2p Depends on Erv14p, an ER–Vesicle Protein Related to the *Drosophila cornichon* Gene Product

Jacqueline Powers and Charles Barlowe

Department of Biochemistry, Dartmouth Medical School, Hanover, New Hampshire 03755

Abstract. COPII-coated ER-derived transport vesicles from *Saccharomyces cerevisiae* contain a distinct set of membrane-bound polypeptides. One of these polypeptides, termed Erv14p (ER–vesicle protein of 14 kD), corresponds to an open reading frame on yeast chromosome VII that is predicted to encode an integral membrane protein and shares sequence identity with the *Drosophila cornichon* gene product. Experiments with an epitope-tagged version of Erv14p indicate that this protein localizes to the ER and is selectively packaged into COPII-coated vesicles. Haploid cells that lack Erv14p are viable but display a modest defect in bud site selection because a transmembrane secretory protein, Axl2p, is not efficiently delivered to the cell surface. Axl2p is required for selection of axial growth

sites and normally localizes to nascent bud tips or the mother bud neck. In *erv14Δ* strains, Axl2p accumulates in the ER while other secretory proteins are transported at wild-type rates. We propose that Erv14p is required for the export of specific secretory cargo from the ER. The polarity defect of *erv14Δ* yeast cells is reminiscent of *cornichon* mutants, in which egg chambers fail to establish proper asymmetry during early stages of oogenesis. These results suggest an unforeseen conservation in mechanisms producing cell polarity shared between yeast and *Drosophila*.

Key words: ER • Golgi • vesicles • coat proteins • cell polarity

SECRETORY proteins destined for intracellular organelles or the plasma membrane are first synthesized and processed at the ER of eukaryotic cells. Fully folded secretory proteins are then packaged into ER-derived transport vesicles for export to the Golgi complex and beyond. Several lines of experimental evidence indicate mechanisms of protein retention and retrieval operate during ER–Golgi transport to maintain distinct organelle identity (Sato et al., 1996; Kaiser et al., 1997). In addition, secretory proteins that must move forward are concentrated into ER-derived vesicles during export from this compartment (Quinn et al., 1984; Balch et al., 1994; Rexach et al., 1994); however, the mechanisms of this selection procedure remain obscure. One component of this selective export process is a protein complex, termed COPII, that forms ER-derived transport vesicles and selects secretory proteins by direct or indirect interaction (Barlowe et al., 1994; Kuehn et al., 1998). In the yeast *Saccharomyces cerevisiae*, formation of ER-derived vesicles has been reconstituted in a cell-free reaction with ER membranes and purified COPII proteins (Salama et al., 1993). We have proposed that additional components of

this selection machinery are contained on ER-derived vesicles, and we have undertaken a molecular analysis of protein constituents on purified COPII-coated vesicles (Belden and Barlowe, 1996).

An uncoated form of ER-derived vesicles may be isolated after centrifugation on density gradients. These gradient-purified vesicles contain a set of tightly associated polypeptides that are solubilized by detergents but not by an elevated pH treatment. NH₂-terminal polypeptide sequences have been determined from several of the abundant species contained on ER vesicles (Ervs),¹ starting with the lowest molecular weight species moving upward (Belden and Barlowe, 1996). In this report, we characterize Erv14p, an integral membrane protein that localizes to the ER and Golgi compartments of yeast cells. Strains that lack Erv14p (*erv14Δ*) are viable but display novel phenotypes in both haploid and diploid stages of growth. First, haploid *erv14Δ* strains are defective in selecting the proper bud site. Wild-type budding yeast are highly polarized during vegetative growth, orienting cytoskeletal elements and the secretory pathway toward the emerging bud tip (Drubin et al., 1991). Haploids select bud sites such that mother and daughter cells bud toward each other and

Address all correspondence to Charles Barlowe, Department of Biochemistry, Dartmouth Medical School, Hanover, NH 03755. Tel.: (603) 650-6516. Fax: (603) 650-1353. E-mail: barlowe@dartmouth.edu

1. *Abbreviations used in this paper:* CPY, carboxypeptidase Y; Endo H, endoglycosidase H; Erv, ER vesicle; HA, hemagglutinin; PMA, plasma membrane ATPase.

therefore exhibit an “axial” budding pattern. Genetic analyses in yeast have led to the identification of several genes that are required for selection of axial growth sites (Chant, 1996). One of these gene products, Axl2p, is an integral membrane secretory protein that must be delivered to the plasma membrane for establishment of the axial bud site (Halme et al., 1996; Roemer et al., 1996). In *erv14Δ* strains, Axl2p is largely retained in the ER and the yeast bud in a nonaxial manner. The accumulation of Axl2p in the ER appears to be selective since other secretory proteins examined were transported at wild-type rates. Second, diploid *erv14Δ/erv14Δ* strains display normal diploid budding patterns but do not sporulate when deprived of nutrients. This sporulation defect does not appear to be related to transport of Axl2p and suggests that Erv14p participates in the transport of additional secretory proteins.

Erv14p shares a high degree of amino acid identity (36%) with the *cornichon* gene product from *Drosophila melanogaster*. Mutations in the *cornichon* gene are known to disrupt anterior–posterior pattern formation during early stages of *Drosophila* oogenesis and ultimately lead to misorientation of the oocyte cytoskeleton (Roth et al., 1995). This phenotype is in some respects similar to the *erv14Δ* phenotype. Therefore, experiments with the yeast homologue of *cornichon* may provide insight on the molecular mechanisms establishing polarity in the *Drosophila* oocyte and perhaps in a variety of cell types.

Materials and Methods

Yeast Strains and Media

The strains used in this study are listed in Table I. Cultures were grown in

either rich medium (1% Bacto-yeast extract, 2% Bacto-peptone, and 2% dextrose [YPD]) or minimal medium (0.67% nitrogen base without amino acids, 2% dextrose [YMD]) containing appropriate supplements. Cultures were grown at 30°C unless indicated differently in figure legends. Standard yeast genetic methods used in these studies have been previously described (Sherman, 1991). Manipulation of recombinant DNA was performed as described (Ausubel et al., 1987), and *Escherichia coli* strain DH5α (Woodcock et al., 1989) was used for these procedures.

Plasmid Construction

The sequence of *ERV14* and its upstream and downstream regions were obtained from the yeast genome database for YGL054c (Feuermann et al., 1997). *ERV14* was isolated by PCR amplification of genomic DNA prepared from *S. cerevisiae* strain FY23 (Winston et al., 1995) using the primers GP3 (5'-CGGAATTCCGGGGTTCCGACTCCCCG-3') and GP4 (5'-CGGGATCCTATTACCGATATTCACCGG-3'). The restriction sites EcoRI and BamHI were used to subclone *ERV14* (including 250 bp upstream and downstream of the open reading frame) into the EcoRI and BamHI sites of pRS316 to produce pRS316-*ERV14*. This construct was sequenced to confirm proper synthesis during amplification. An epitope tag corresponding to the hemagglutinin (HA) peptide sequence YPYD-VPDYA (Wilson et al., 1984) was added on the COOH terminus of Erv14p and was synthesized using the primers GP3 and JP11 (5'-TCC-CCGCGGTTAAGCGTAGTCTGGGACGTCGTATGGGTAGAAGT-CATCACCACCTTTCAGC-3'). This primer anneals to the 3'-coding sequence of *ERV14* and inserts the HA epitope followed by a stop codon and a SacII restriction site. The resulting ~700-bp PCR product was treated with EcoRI and SacII and then ligated into the EcoRI/SacII site of pRS316. The 3' untranslated region for *ERV14* was restored by inserting the 340-bp PCR product synthesized using the primers JP12 (5'-TCC-CCGCGGTCCAACAAGACATTGAAATCC-3') and JP13 (5'-AGG-CCGCGGATTTACAGTCATGCTCACCC-3') into the SacII site. This construct (pRS316-*ERV14HA*) was sequenced to confirm proper synthesis during amplification.

Strain Construction

The *ERV14* locus was targeted for disruption with the *HIS3* gene (Baudin et al., 1993). A PCR method was used to amplify an *erv14::HIS3* disruption fragment using the primers GP1 (5'-TGCAATTAAGTAAAG-

Table I. Strain List

Strain	Genotype	Reference
FY833	<i>MATa his3Δ200 ura3-52 leu2Δ1 lys2Δ202 trp1Δ63</i>	Winston et al. (1995)
FY834	<i>MATα his3Δ200 ura3-52 leu2Δ1 lys2Δ202 trp1Δ63</i>	Winston et al. (1995)
RSY263	<i>MATα sec12-4 ura3-52 leu2-3,112</i>	Kaiser and Schekman (1991)
CBY251	<i>MATα his3Δ200 ura3-52 leu2Δ1 lys2Δ202 trp1Δ63 erv14::HIS3</i>	This Study
CBY347	<i>MATa his3Δ200 ura3-52 leu2Δ1 lys2Δ202 trp1Δ63 erv15::TRP1</i>	This Study
CBY348	CBY251 × CBY347	This Study
CBY353	<i>MATα his3Δ200 ura3-52 leu2Δ1 lys2Δ202 trp1Δ63 erv15::TRP1</i>	This Study
CBY354	<i>MATα his3Δ200 ura3-52 leu2Δ1 lys2Δ202 trp1Δ63 erv14::HIS erv15::TRP1</i>	This Study
CBY355	<i>MATa his3Δ200 ura3-52 leu2Δ1 lys2Δ202 trp1Δ63</i>	This Study
CBY356	<i>MATα his3Δ200 ura3-52 leu2Δ1 lys2Δ202 trp1Δ63 erv14::HIS3</i>	This Study
CBY358	<i>MATa his3Δ200 ura3-52 leu2Δ1 lys2Δ202 trp1Δ63 erv14::HIS3</i>	This Study
CBY407	CBY354 containing <i>pRS316-ERV14HA</i>	This Study
CBY409	CBY356 containing <i>pRS316-ERV14HA</i>	This Study
CBY410	CBY356 × CBY358	This Study
CBY432	CBY410 containing <i>pRS316</i>	This Study
CBY433	CBY410 containing <i>pRS316-ERV14HA</i>	This Study
CBY435	CBY411 containing <i>pRS316-ERV14HA</i>	This Study
CBY453	FY833 × FY834	This Study
CBY460	CBY355 containing <i>p2μm-AXL2</i>	This Study
CBY461	CBY355 with <i>AXL2::3XHA</i>	This Study
CBY462	CBY356 containing <i>p2μm-AXL2</i>	This Study
CBY463	CBY356 with <i>AXL2::3HA</i>	This Study
CBY464	CBY410 containing <i>p2μm-AXL2</i>	This Study
CBY471	RSY263 with <i>AXL2::3HA</i>	This Study
CBY477	CBY356 containing <i>pRS316</i>	This Study
CBY508	CBY356 containing <i>pRS316-ERV14</i>	This Study

TAAAAAATTAAGAATAAAAAAGAAAAGGCCTCTCTAGTACTACT-3') and GP2 (5'-CTTGGCCCTTCAGTCTTCTTTGGATTTC-AATGTCTTGTGGAGCGCGCCTCGTTCAGAATG-3') with pHISKO as a template. The resulting product has the *HIS3* gene flanked by 45 bp of the *ERV14* gene directly before the ATG start and directly after the stop codon. Transformation of strain YPH501 (Sikorski and Heiter, 1989) to histidine prototrophy and subsequent screening identified several isolates that were heterozygous at the *ERV14* locus. Several of these heterozygous diploids were grown under conditions to induce sporulation, and dissection of these asci produced four viable spores. A haploid disruptant (CBY251) was also constructed in strain FY834 and used in subsequent studies. Disruption of the *ERV14* locus was confirmed by two independent PCR analyses. First, the GP3 primer and a primer internal to the *HIS3* gene (5'-GCCTCATCCAAAGGCGC-3') generated a product (650 bp) of the expected size, and second, primers that flank the *ERV14* gene (GP3 and GP4) produced a single product (1,500 bp) of the expected size.

An *Erv14p* homologue that shares 63% amino acid identity is defined by open reading frame YBR210w on chromosome II (Feldmann et al., 1994), referred to here as *ERV15*, and was also targeted for disruption with the *TRP1* gene in a multistep procedure. The primers EF4 (5'-AATCTAGAGCTCACTACTCTCTC-3') and EF3 (5'-AAACTC-GAGCAAATACGAGGGAGATCG-3'), which correspond to regions that are ~210 bp upstream and ~300 bp downstream of the open reading frame, were used to amplify *ERV15* from genomic DNA. These primers contain the restriction sites *Xba*I (EF4) and *Xho*I (EF3) to facilitate insertion into the homologous sites of pRS305 (Sikorski and Heiter, 1989). This plasmid, pREF305, was modified to disrupt the open reading frame of *ERV15* with *TRP1*. A unique *Pst*I site located 29 bases upstream of the *ERV14* start codon and a partial digest of *Dra*I (site is located 328 bp downstream from the ATG start) were used to insert the *TRP1* gene. A *Pst*I/*Sma*I digest of pJJ248 (Jones and Prakash, 1990) liberates a 955-bp fragment containing the *TRP1* gene that was then inserted into pREF305 treated with *Pst*I and *Dra*I. The resulting plasmid, pEFT305, was digested with *Not*I/*Xba*I, and the 1.6-kbp fragment containing the *TRP1* gene flanked by *ERV15* sequence was isolated. This disruption fragment was used to transform strain FY833. Tryptophan prototrophs were screened using the primers EF7, 5'-CTGAACGACAAAGTGAAGC-3' (anneals 404 bp downstream of the *ERV15* stop codon) and JP7, 5'-TCACCTGTCCACCTGC-3' (anneals 500 bp downstream from the *TRP1* start codon), which produce a 1.1-kbp amplification product if integration has occurred at the *ERV15* locus. One of these isolates, CBY347, was used in subsequent experiments and was mated with CBY251 to generate the double *erv14::HIS3 erv15::TRP1* strain, CBY348. This strain was placed in media to induce sporulation, and an isogenic set of strains containing the single and double disruptions (CBY353, CBY354, CBY355, and CBY356) were isolated for use in these studies. To prepare diploids homozygous for *erv14::HIS3*, CBY356 was mated with CBY358, and zygotes were picked by their distinctive morphology under the microscope.

Antibodies and Immunoblotting

Antibodies directed against Sec61p (Stirling et al., 1992), Sec22p (Bednarek et al., 1995), *Erv25p* (Belden and Barlowe, 1996), *Emp47p* (Schröder et al., 1995), Sec23p (Hicke and Schekman, 1989), *Kar2p* (Brodsky and Schekman, 1993), *CPY* (Rothblatt et al., 1989), *Gas1p* (Frankhauser and Conzelmann, 1991), *Vph1* (Kane et al., 1992), and plasma membrane ATPase (Carolyn Slayman, Yale University, New Haven, CT) were used in these studies. Anti-HA monoclonal antibody (HA.11) raised against the peptide CYPYDVPDYASL was obtained from Berkeley Antibody Co. (Richmond, CA). Polyclonal antiserum specific for Sec12p was raised against the NH₂-terminal domain of Sec12p (amino acid residues 1–354) fused to protein A. Fusion protein was expressed from the plasmid pRIT33 (Nilsson and Abrahmsen, 1990) and purified by IgG affinity chromatography as described by the manufacturer (Pharmacia Biotech, Piscataway, NJ). Antigen (0.25 mg) was mixed with Freund's complete adjuvant and injected into rabbits followed by monthly boosts with 0.12 mg of antigen in Freund's incomplete adjuvant. Serum isolated from immunized rabbits cross-reacted with a 70-kD species that was overproduced when transformed with a *GALI*-regulated version of *SEC12* (d'Enfert et al., 1991). For immunoblots, proteins were resolved by SDS-PAGE (Laemmli, 1970) and transferred to nitrocellulose (Towbin et al., 1979), and filter-bound primary antibodies were detected by peroxidase-catalyzed chemiluminescence (ECL method; Amersham Corp., Arlington Heights, IL).

In Vitro Vesicle Budding

Microsomes were isolated from strain CBY409 and incubated in the presence or absence of proteins required for reconstitution of vesicle formation as described (Barlowe et al., 1994). A 15- μ l portion of the total reaction and 150 μ l of a supernatant fluid containing vesicles released from 200- μ l budding reactions were centrifuged at 100,000 g (model TLA100.3 rotor; Beckman Coulter, Inc., Fullerton, CA) to collect membranes. The pellet fractions were dissolved in 30 μ l of SDS-PAGE buffer, and 7–10 μ l of this material was resolved on 12.5% polyacrylamide gel and immunoblotted for Sec22p, *Erv25p*, Sec12p, and anti-HA for *Erv14p*-HA detection.

Subcellular Fractionation

Subcellular fractionation was performed as described by Antebi and Fink (1992) with modifications by Schimmöller et al. (1995). Strains were grown to exponential phase and converted to spheroplasts by lyticase treatment (Baker et al., 1988). Spheroplasts were centrifuged and resuspended in a sucrose solution (10 mM Hepes, pH 7.5, 12.5% sucrose, 1 mM EDTA, 1 mM PMSF) and subjected to 10 strokes in a Dounce homogenizer. Two clearing spins were performed, and the resulting supernatant fluid was placed on a sucrose gradient consisting of nine steps from 22 to 60% (wt/vol) in 10 mM Hepes, pH 7.4, 1 mM MgCl₂. The gradients were centrifuged at 35,000 rpm (model SW40 rotor; Beckman Instruments, Palo Alto, CA) for 2.5 h at 4°C. 15 fractions of 0.77 ml each were taken sequentially from the top of the gradient to the bottom. Fractions were diluted in SDS-PAGE sample buffer, and proteins were resolved on polyacrylamide gels and immunoblotted for Sec61p (ER marker), *Emp47p* (Golgi marker), plasma membrane ATPase (PMA), *Vph1* (vacuolar marker), and anti-HA monoclonal antibody to detect *Erv14p*-HA or *Axl2*-HA. Relative levels of specific proteins in each fraction were quantified by densitometry of immunoblots. GDPase activity was determined as described (Yanagisawa et al., 1990) using CDP to subtract nonspecific phosphatase activity. Sucrose concentrations of individual fractions were determined by measuring the refractive index with an Abbe Refractometer (American Optical, Buffalo, NY).

For subcellular fractionation under conditions of divalent cation chelation, the method of Kölling and Hollenberg (1994) was followed. Cells were grown and spheroplasted as described above; however, lysates were prepared by agitation with glass beads in buffer containing 10 mM Hepes, pH 7.5, 12.5% sucrose, 10 mM EDTA, 1 mM PMSF. The cleared lysate was loaded onto a similar 22–60% sucrose gradient as described above, except gradients contained 10 mM EDTA, and samples were centrifuged at 30,000 rpm (model SW40 rotor; Beckman Instruments) for 14 h at 4°C. Fractions were collected and analyzed as described above for magnesium-containing gradients.

To characterize the membrane association of *Erv14p*, yeast cell membranes were isolated and treated with various agents as follows. Spheroplasts were prepared as indicated above and resuspended in buffer 88 (20 mM Hepes, pH 6.8, 250 mM sorbitol, 150 mM KOAc, 5 mM MgOAc) containing 1 mM DTT and 1 mM PMSF. After Dounce homogenization, a low-speed supernatant fraction was prepared by centrifugation at 5,000 rpm (model SS34 rotor; Sorvall, Newtown, CT). Aliquots from the supernatant fraction were treated with buffer 88, 0.5 M NaCl, 2.5 M urea, 0.1 M sodium carbonate, or 1% Triton-X 100 in buffer 88. These samples were mixed and incubated 20 min on ice followed by centrifugation at 60,000 rpm (model TLA 100.3 rotor; Beckman Instruments) for 15 min. Equivalent amounts of supernatant and pellet fractions were diluted in SDS-PAGE buffer and resolved on a 12.5% polyacrylamide gel. Blots were probed with anti-*Emp47p* (integral membrane protein), anti-Sec23p serum (peripheral membrane protein), or anti-HA monoclonal antibody to detect *Erv14p*-HA.

Calcofluor Staining of Bud Scars

Yeast strains in a logarithmic stage of growth were diluted into YPD medium to an OD₆₀₀ of 0.002. When cultures reached an OD₆₀₀ of 0.5–0.8, an aliquot (1.5 ml) of cells was harvested and resuspended in calcofluor stain at a concentration of 0.1 mg/ml, as described (Pringle, 1991). After incubation for 5–10 min at room temperature, the cells were washed three times in distilled water and resuspended in a final volume of 50 μ l. Stained yeast were viewed under a fluorescence microscope, and cells possessing six or more bud scars were examined for an axial or nonaxial budding pattern. Haploid cells that displayed one or more bud scars at opposite poles were scored as nonaxial.

Sporulation and Cell Survival Experiments

Sporulation efficiency and cell survival studies were performed as follows. Diploid strains were cultured for 8 h at 30°C in YPD to an exponential phase of growth. Cells were then harvested, washed twice with water, and resuspended to an OD₆₀₀ of 1 in spmD, a nitrogen-deficient medium composed of 1% potassium acetate, 0.1% yeast extract, and 0.05% dextrose. To assess sporulation efficiency, samples from these cultures were microscopically examined daily to determine the number of tetrads per 300 cells. Cell viability from these cultures was assessed over a 7-d period by spreading an equivalent amount of OD₆₀₀ units on YPD plates. After 4 d of growth on YPD plates, the colonies were counted to determine cell viability.

Indirect Immunofluorescence

Yeast strains were grown in 25 ml of YPD to an OD₆₀₀ of 0.3 and fixed with 5% formaldehyde for 1 h. Fixed cells were then centrifuged for 3 min in a clinical centrifuge, washed three times in PBSS (PBS, pH 7.4, and 0.7 M sorbitol) and resuspended in a final volume of 400 µl PBSS. β-Mercaptoethanol (20 mM final) and lyticase were added and incubated at room temperature for 30 min to digest cell walls. The fixed spheroplasts were washed twice and resuspended in 400 µl of PBSS, and 15 µl was applied to polylysine-coated multiwell slides (Pringle et al., 1991). Cells were adhered for 10 min, washed, and incubated with blocking buffer (PBSS with 1% BSA and 0.5% Triton X-100) for 10 min. Wells were washed twice with PBSS followed by the addition of primary antibodies (anti-Kar2p at 1:500 and anti-HA at 1:200) diluted in blocking buffer. After incubation at room temperature for 90 min, cells were washed five times with PBSS and then incubated with secondary antibodies that had been diluted in blocking buffer at 1:500 (anti-rabbit IgG conjugated to fluorescein or anti-mouse IgG conjugated to Texas red). After 90 min, cells were washed four times with PBSS followed by a 1-min incubation in PBSS containing 1 µg/ml diamidophenylindole. Cells were then washed four times with PBSS, and mounting medium (FITC guard; Testog, Inc., Chicago, IL) was layered on wells before sealing with coverslips. For all fluorescence microscopy, images were obtained using a cooled CCD camera, and composites were prepared with Adobe Photoshop (San Jose, CA) software.

In Vivo Labeling

Pulse-chase experiments were performed as previously described (Belden and Barlowe, 1996). In brief, cells were grown at 30°C (25°C for the *sec12-4* strain) in selective medium containing 2% dextrose to an OD₆₀₀ of 0.5. Cultures were harvested, washed, and resuspended at one-tenth the original volume in selective medium lacking sulfate. After culturing for 10 min at 30°C (37°C for *sec12-4* strain), cultures were pulsed for 10 min by the addition of [³⁵S]Express label (NEN™ Life Science Products, Boston, MA) and chased by the addition of excess methionine and cysteine. Cell samples were taken at the end of the pulse period and after 10 and 20 min of chase. Cell lysates were prepared by bead-beat lysis, and labeled species were precipitated from a common extract with specific antibodies for CPY, Gas1p, or anti-HA monoclonal antibody that recognizes Axl2p-HA. For endoglycosidase H (Endo H) experiments, 20-min chase time points were taken, and Axl2p-HA was immunoprecipitated in duplicate from indicated strains. Washed immunoprecipitates were equilibrated with 100 mM sodium citrate, pH 5.5, and one tube of each duplicate was incubated with 5 mU of Endo H (Sigma Chemical Co., St. Louis, MO) for 12 h at 37°C. Samples were resolved on 7.5 or 10% polyacrylamide gels, and labeled species were visualized by fluorography.

Results

Identification of Erv14p

Uncoated ER-derived vesicles were isolated, and vesicle proteins were resolved on a 15% polyacrylamide gel as previously described (Belden and Barlowe, 1996). Approximately 0.02 mg of the 14-kD protein was purified and subjected to automated NH₂-terminal sequencing. The sequence GAWLFILAVVVNINLFG was obtained from the polypeptide corresponding to Erv14p (X represents a residue that could not be unambiguously determined).

A

```
Erv14p:  MGAWLFILAVVVNINLFGQVHFTLLYADLEADYINPTIELCSKV (44)
          A + I+A++ + +F + I + +L+ DY NPI+ C+ +
cni:     MAFNFTAFTYIIVALIGDAFLIFFAIFHVIAPDELKTDYKNPIDQCNSL (48)

(45)    NKLLITPEAALHGALSLLFLLNGYVWFVFLNLPVLAAYLNKIKYK-VQ (90)
          N L+ PE LH L+LLFL G WF +N+P++AY++ + N+ V
(49)    NPLVLPPEYLLHIFLNLFLFCGGEWFSLCINIPLIAYHIWRYKRPVM (95)

(91)    LLDATEIFR--TLGKHKRESFLKLGPHLLMFFFYLYRMIMALIAESGDDP (138)
          L D T + + TL ++ RE ++KL +L+ FF+Y+Y M+ +LI+ +
(100)   LYDPTTLVKTDTLYRNMRREGWIKLAVYLLISFFYYIYGMVYSLIS-T (144)
```

B

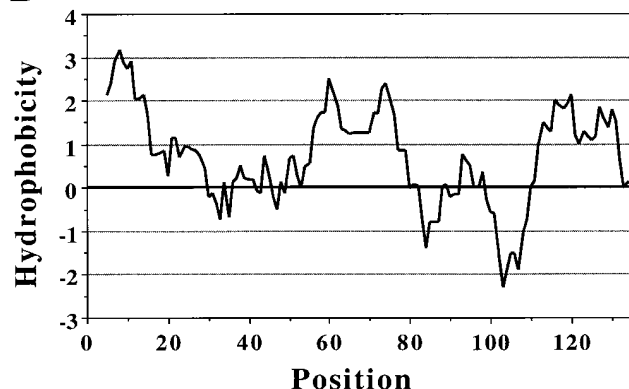
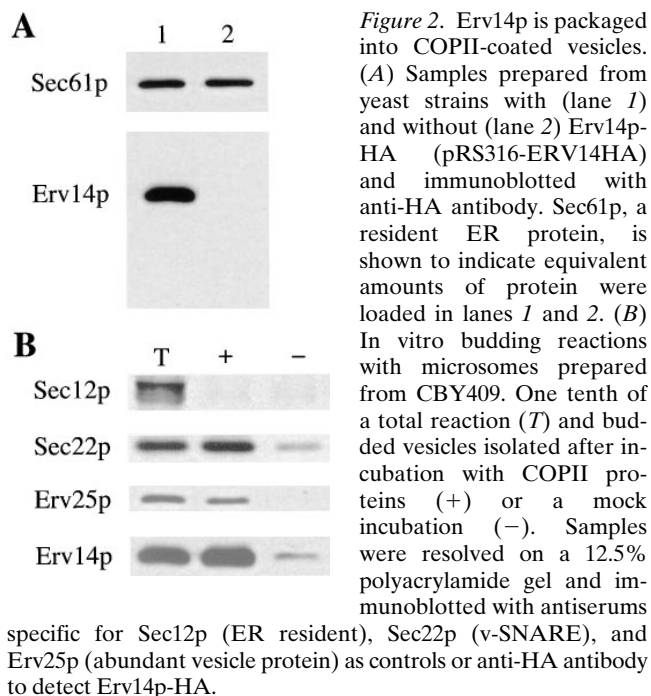


Figure 1. (A) Predicted amino acid sequence of Erv14p with underlined amino acids to indicate NH₂-terminal residues sequenced. Shown below is the predicted *cornichon* (*cni*) polypeptide sequence with amino acid identities and similarities (+) indicated. (B) Hydrophobicity plot as described (Kyte and Doolittle, 1982).

The NH₂-terminal sequence of Erv14p (Fig. 1 A, underlined) aligns with an unidentified open reading frame on chromosome VII (YGL054c) reported by the yeast genome sequencing project (Feuermann et al., 1997). Conceptual translation of YGL054c produces a 138-amino acid protein that contains three segments of sufficient length and hydrophobicity to span a lipid bilayer. Based on this sequence information and further data presented in this report, Erv14p is likely an integral membrane protein. A search of the current protein database identified a 142-amino acid unidentified open reading frame in *S. cerevisiae*, YBR210w (Feldmann et al., 1994), which shares 63% identity with Erv14p, and the predicted 144-amino acid *cornichon* gene product from *Drosophila melanogaster*, which shares 36% identity. Other than these sequence homologies, Erv14p does not contain consensus sites for N-linked glycosylation or any characterized sequence motifs to provide insight into molecular function.

Erv14p Is an Integral Membrane Protein Localized to the ER and Golgi

To investigate Erv14p function and location, the molecular clone was modified to express a nine-amino acid influenza HA-epitope at the extreme COOH terminus that is recognized by a monoclonal antibody HA.11 (see Materials and Methods). Yeast cells harboring this Erv14p-HA expression vector on a centromere (CEN)-based plasmid



produced an ~15-kD immunoreactive species that was absent in untransformed strains (Fig. 2 A). Experiments described in later sections (for example Table I) demonstrate that Erv14p-HA complements the phenotypes displayed by an *erv14Δ* strain and indicate that this tagged version is fully functional. For the experiments described in this section, CBY409 was constructed such that Erv14p-HA is expressed from a CEN plasmid in an *erv14Δ* strain to keep the concentration of Erv14p-HA near normal cellular levels.

First, we isolated COPII vesicles from in vitro reactions using ER membranes prepared from the Erv14p-HA-tagged strain CBY409. If Erv14p is an authentic Erv protein, it should be selectively packaged into vesicles only when COPII proteins are included in the incubation. Under reconstituted budding conditions (Fig. 2 B), ER-derived vesicles incorporated Erv14p-HA at a level (~12%) comparable to other characterized vesicle proteins, such as Sec22p (Barlowe et al., 1994; Rexach et al., 1994) and Erv25p (Belden and Barlowe, 1996). Resident ER proteins, such as Sec12p and Sec61p (not shown), were not packaged into COPII-coated vesicles under these conditions. In this experiment, [³⁵S]glycylpro-α-factor was released at an efficiency of 23% in the presence of COPII proteins and 3% in their absence. Thus, Erv14p satisfies the initial criteria of an Erv protein such that this species is selectively exported from ER membranes under conditions that reconstitute vesicle budding.

Next, we investigated the nature of Erv14p association with membranes. The predicted amino acid sequence for Erv14p suggests this protein spans the lipid bilayer three times and is consistent with the result that several of the Erv proteins (including an ~14-kD species) partition to a carbonate inextractable pellet fraction (Rexach et al., 1994). The fractionation behavior of Erv14p-HA was monitored (Fig. 3) under conditions that extract peripherally bound membrane proteins (2 M urea), release lumenal

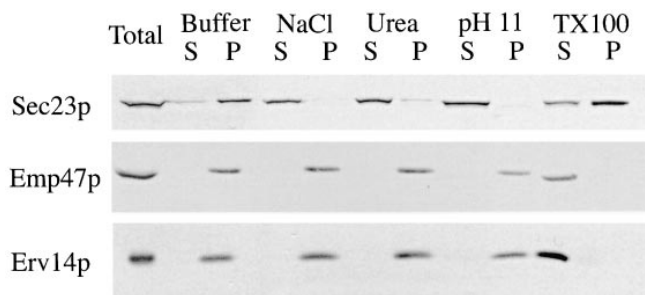


Figure 3. Erv14p is an integral membrane protein. Yeast cell lysates prepared from CBY409 were treated (see Materials and Methods) with buffer, buffer containing 0.5 M NaCl, 2.5 M urea, 0.1 M Na₂CO₃, pH 11, or 1% Triton X-100, and then centrifuged at 100,000 g. The resulting supernatant fluid (S) or pellet (P) fractions were resolved on 12.5% polyacrylamide gels and immunoblotted for Emp47p (integral membrane protein), Sec13p (peripheral membrane protein), or anti-HA to detect Erv14p-HA.

proteins (0.1 M Na₂CO₃, pH 11), or solubilize integral membrane proteins (1% Triton X-100). The fractionation profile of Erv14p-HA was identical to an integral membrane protein such as Emp47p (Schröder et al., 1995) and not the peripheral membrane protein Sec23p (Hicke and Schekman, 1989). We conclude that Erv14p is an integral membrane protein. Application of the “positive inside” rule (von Heijne and Gavel, 1988) suggests a topology such that the NH₂ terminus is oriented toward the cytoplasm and the COOH terminus is oriented toward the luminal compartment.

Previous experiments demonstrated that cycloheximide pretreatment does not diminish the level of abundant Erv proteins contained on COPII-coated vesicles (Yeung et al., 1995). This condition depletes ER membranes of known secretory proteins but does not inhibit in vitro synthesis of COPII-coated vesicles. Based on this observation, we hypothesize that the abundant Erv proteins, including Erv14p, are not newly made secretory proteins en route to the Golgi complex. Instead, we propose that many of the Erv proteins are structural components of COPII-coated vesicles and cycle between the ER and Golgi, functioning in aspects of vesicle budding or fusion (Belden and Barlowe, 1996). The following experiments indicate Erv14p localizes to the ER and Golgi compartments and suggest that Erv14p is not an abundant secretory protein. First, whole-cell immunofluorescence (Fig. 4) with an Erv14p-HA strain (CBY409) revealed a distinct perinuclear staining pattern for Erv14p-HA, much of which was coincident with that observed for the ER-resident protein Kar2p/BiP (Rose et al., 1989). A distinct staining pattern was not detected using the anti-HA antibody in strains lacking the Erv14p-HA construct, indicating a specific signal from the HA epitope (data not shown). Second, fractionation of membranes isolated from CBY409 on sucrose gradients (Antebi et al., 1992) showed that ~70% of Erv14p-HA cosediments with the ER marker Sec61p and ~30% cosedimented with the Golgi marker Emp47p (Fig. 5). This subcellular distribution is similar to other vesicle proteins (Emp24p and Erv25p) that appear to cycle between the ER and Golgi compartments (Schimöller et al., 1996; Belden, W.J., and C. Barlowe, manuscript in preparation).

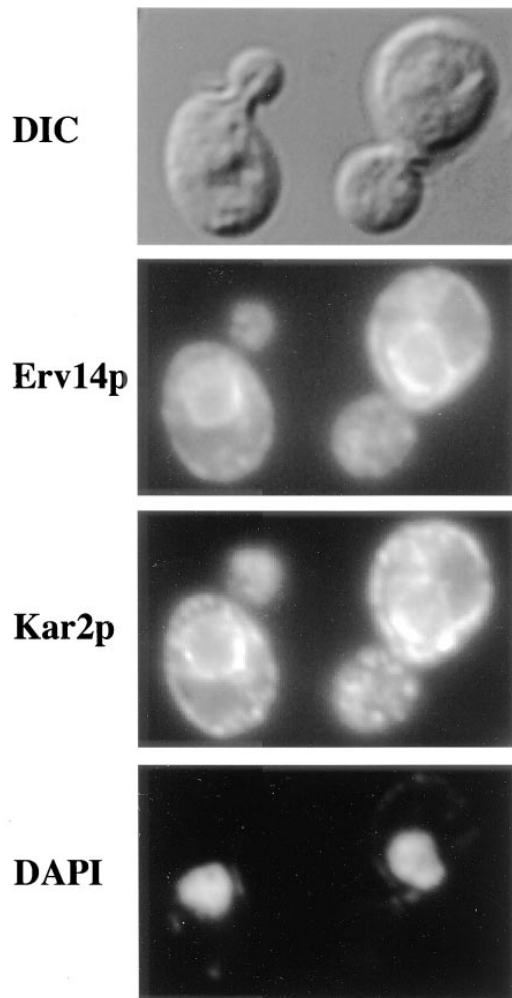


Figure 4. Erv14p localizes to perinuclear regions. Double-label immunofluorescence microscopy of CBY409 cells using Kar2p antiserum and anti-HA monoclonal antibody for Erv14p-HA detection. Differential interference contrast (DIC) indicates cell boundaries and diamidophenylindole (DAPI) stains nuclei. Note significant overlap in staining pattern of the ER-resident protein Kar2p and Erv14p-HA.

Erv14p Is Required for an Axial Budding Pattern in Haploid Cells

To characterize the function of Erv14p, we analyzed a yeast strain bearing a null allele at the *ERV14* chromosomal locus. Oligonucleotides corresponding to 3' and 5' regions of *ERV14* and *HIS3* were used to direct *HIS3* to the *ERV14* locus, thereby replacing the open reading frame of Erv14p from start to stop codons. A heterozygous diploid (*ERV14/erv14Δ*) was obtained and sporulated, and dissection of individual asci produced four viable spores. Analysis of these spores by growth on different selective media and PCR amplification to confirm disruption indicated that *ERV14* was dispensable for vegetative growth (data not shown). Strains carrying the null allele grew at rates identical to wild-type strains and were not thermosensitive. Although the logarithmic phase growth rate of *erv14Δ* strains was wild-type, we found that *erv14Δ* strains exhibited a prolonged lag phase when diluted from

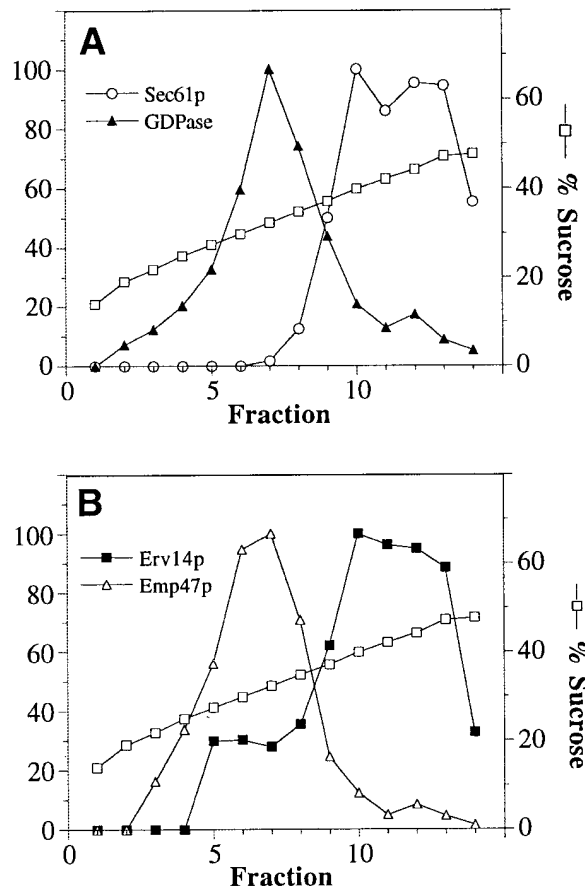


Figure 5. Sucrose gradient fractionation of Erv14p-HA. A whole cell lysate from strain CBY409 was separated on a sucrose density gradient (20–60%) and fractions collected from the top. Relative levels of Sec61p (ER marker), Emp47p (Golgi marker), and Erv14p-HA in each fraction were quantified by densitometry of immunoblots. GDPase (Golgi marker) was measured by enzymatic assay.

stationary phase cultures into standard rich media such as YPD (see Materials and Methods). The lag phase delay was further exacerbated when diluted into yeast minimal media such as YMD. This growth phenotype was linked to the *HIS3* disruption of *ERV14* and was corrected when transformed with a plasmid containing the *ERV14* gene.

Erv14p shares amino acid identity with the *Drosophila cornichon* gene product over the entire open reading frame, and their hydrophobicity profiles are superimposable. The *cornichon* gene is necessary for establishment of anterior–posterior asymmetry during early stages of oogenesis (Ashburner et al., 1990; Roth et al., 1995); however, a molecular determination of *cornichon* gene product function has not been reported. We used this clue of *cornichon* function in generating cellular asymmetry to explore a possible role for Erv14p in yeast cell polarity. *S. cerevisiae* undergoes polarized cell growth such that the plane of cell division is determined by the site of bud formation and is dependent on cell type. Haploid yeast bud in an axial manner, placing each new bud adjacent to the previous bud site. Genetic analysis of bud site selection has revealed a group of *bud* and *axl* mutants defective in the haploid axial budding pattern. The phenotypes of these

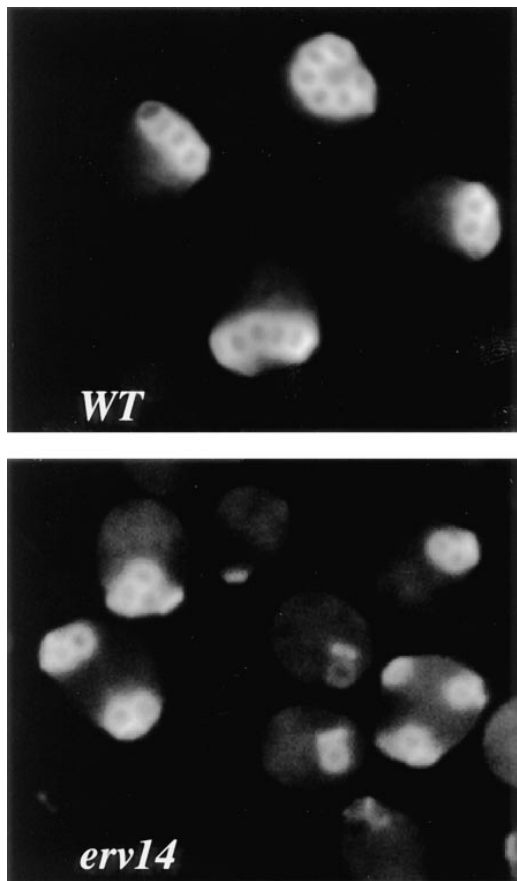


Figure 6. Budding patterns in wild-type (*WT*) and *erv14* strains. Logarithmically grown cells were stained with calcofluor to visualize chitin rings. Wild-type cells display the characteristic axial budding pattern, whereas *erv14* cells exhibit nonaxial budding patterns.

mutants fall into distinct categories, with one group that displays a random bud site selection pattern and a second group that exhibits bipolar patterns instead of the normal axial pattern (Bender and Pringle, 1989; Chant and Herskowitz, 1991; Chant et al., 1991; Fugita et al., 1994; Chant and Pringle, 1995; Halme et al., 1996; Roemer et al., 1996; Sanders and Herskowitz, 1996). A history of bud site selection in yeast may be visualized by staining with calcofluor, a fluorophore that binds to chitin and reveals previous bud scars as chitin-rich rings (Hayashibe and Katohda, 1973). Logarithmic-stage cultures of wild-type and *erv14*Δ

Table II. Budding Pattern of Haploid Cells

Strain	Number of cells exhibiting nonaxial budding/600 cells	Percent nonaxial budding
CBY355 (<i>WT</i>)	3	0.5
CBY356 (<i>erv14</i> Δ)	98	16.3
CBY477 (<i>erv14</i> Δ/ <i>pRS316</i>)	93	15.5
CBY508 (<i>erv14</i> Δ/ <i>pRS316-ERV14</i>)	7	1.2
CBY409 (<i>erv14</i> Δ/ <i>pRS316-ERV14HA</i>)	2	0.3
CBY462 (<i>erv14</i> Δ/ <i>p2μm-AXL2</i>)	40	6.7

Log phase cells with six bud scars or more were evaluated for nonaxial budding patterns. Cells that displayed one or more bud scars at opposite poles were scored as non-axial.

strains were grown in rich medium and stained with calcofluor. Strikingly, *erv14*Δ haploid strains displayed a nonaxial budding phenotype that was not observed in an isogenic wild-type strain (Fig. 6). In a quantitative analysis of bud site selection, the penetrance of this phenotype was incomplete, but a significant fraction of mothers exhibited nonaxial budding patterns (see Table II). Transformation of *erv14*Δ strains with a CEN-based plasmid expressing *Erv14p* or *Erv14p-HA* reversed the nonaxial budding phenotype and confirmed that this defect was caused by deletion of *Erv14p* (Table II). Furthermore, these results indicated *ERV14-HA* is functional and complements as effectively as unmodified *ERV14*.

We also examined the influence of disrupting *YBR210w* on bud site selection. This predicted open reading frame on chromosome II shares 63% amino acid identity with *Erv14p* and could be functionally redundant. Disruption of this gene (*ERV15*) produced viable haploids (CBY347 and CBY353) that displayed no apparent phenotypes. Furthermore, combination of *erv14*Δ with *erv15*Δ (CBY354) did not exacerbate the nonaxial budding pattern displayed by a single *erv14*Δ strain (not shown). We also designed a construct to express an epitope tag on the COOH terminus of *Erv15p*, an approach that had proven successful for detection of *Erv14p*. Although DNA sequencing indicated correct synthesis of this construct, we failed to detect a tagged species under our standard growth conditions (data not shown). To rationalize these observations, we speculate that *ERV15* is not functionally redundant with *ERV14* when cells are grown in rich medium and that *ERV15* expression may be restricted to specific stages of the yeast life cycle.

Wild-type *a/α* diploids exhibit a bipolar budding pattern such that a mother cell may produce a new bud at either pole from the previous bud site. We examined the budding pattern in homozygous diploid strains lacking *Erv14p* (CBY410) and in strains lacking both *Erv14p* and *Erv15p* (CBY411). These strains did not exhibit any alterations in the bipolar positioning of the bud site (data not shown). Therefore, *erv14*Δ strains possess haploid-specific defects in establishing cell polarity, as reported for a subset of the *axl* and *bud* mutants (Chant et al., 1995; Roemer et al., 1996).

Axl2p Accumulates in the ER of *erv14* Mutants

Because *Erv14p* is localized to the early compartments of the secretory pathway, and this pathway is responsible for the delivery of proteins to the plasma membrane, we considered the possibility that *Erv14p* was required for transport of factors to the cell surface for establishment of cell polarity. Combined molecular/genetic approaches have provided a wealth of information on the proteins involved in bud site selection in yeast (for review see Chant, 1996). *Axl2p* is one of the characterized proteins that is required for an axial budding pattern and displays a bipolar phenotype when disrupted in haploid cells. *Axl2p* is also an integral membrane glycoprotein with a predicted type I topology and is known to traverse the secretory pathway en route to the cell surface (Roemer et al., 1996). During the biogenesis of *Axl2p*, N-linked core oligosaccharides are added in the ER and are further extended during passage

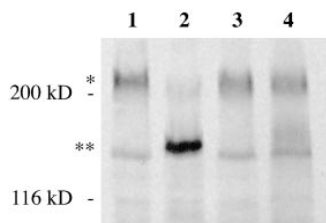


Figure 7. Immunoblot of Axl2p-HA in wild-type and *erv14Δ* strains. Lysates prepared from wild-type strain CBY461 (lane 1), *erv14Δ* strain CBY463 (lane 2), and *sec12* strain CBY471 (lanes 3 and 4) were resolved on a 7.5% polyacrylamide gel. For the *sec12* strain, cells were

grown at 25°C (lane 3) or shifted to 37°C for 2 h (lane 4). Proteins were transferred to nitrocellulose and probed with anti-HA antibodies for Axl2p-HA detection. Note the wild-type form of Axl2p-HA (*) and a faster migrating form of Axl2p-HA (**) observed in the *erv14Δ* strain (lane 2) and the *sec12* strain shifted to a restrictive temperature (lane 4). A faint cross-reactive species migrating just below the faster migrating form of Axl2p-HA is an endogenous protein detected in strains lacking *AXL2::3XHA*.

through Golgi compartments. We tested if Axl2p was efficiently transported in strains carrying an *erv14Δ* allele and used a triple-HA-tagged version of Axl2p (known to complement an *axl2Δ* strain) to monitor transport of Axl2p (Roemer et al., 1996). In an initial experiment, we immunoblotted whole-cell extracts from wild-type and mutant strains expressing Axl2p-3HA (Fig. 7). In an *erv14Δ* null strain, an ~150-kD HA-tagged species that was not detected in wild-type strains was apparent. In contrast, wild-type strains expressed an ~220-kD form that was a very minor species in *erv14Δ* null strains. We reasoned that the 150-kD form of Axl2p-3HA that was unique to the *erv14Δ* strain represented a core-glycosylated form of this secretory protein that may accumulate in the ER. The next series of experiments are focused on this hypothesis.

The temperature-sensitive *sec12-4* allele blocks ER to Golgi transport when shifted to a restrictive temperature, and ER forms of secretory proteins accumulate (Novick et al., 1980; Stevens et al., 1984). Sec12p is an integral membrane glycoprotein localized to the ER, and it is required for the formation of transport vesicles from this compartment (Nakano et al., 1988; d'Enfert et al., 1991). We transformed a *sec12-4* strain with the Axl2p-3HA expression construct to monitor the ER form of Axl2p-3HA that accumulates when shifted to a restrictive temperature. Under steady-state conditions (Fig. 7, lane 3), the 150-kD form of Axl2p-3HA was not detected; however, after a shift to 37°C for 2 h, a small amount of this species became apparent in a *sec12-4* strain (Fig. 7, lane 4).

The above experiments suggest that Axl2p-3HA accumulates in the ER as a 150-kD core-glycosylated form in *erv14Δ* and *sec12-4* strains. The immunoblot experiments provide a steady-state view of Axl2p-3HA in these strains. However, we sought to characterize the kinetics of Axl2p-3HA transport in wild-type and *erv14Δ* strains through a pulse-chase analysis. In these experiments, cells were grown in minimal medium and pulsed with [³⁵S]methionine and cysteine for 10 min to label newly synthesized proteins. Excess cold methionine and cysteine were then added to initiate the chase phase, and the fate of specific secretory proteins (Axl2p-3HA, CPY, and Gas1p) were monitored by selective immunoprecipitation of these species from whole-cell lysates (Fig. 8). CPY is first detected

in the ER as the P1 precursor (67 kD), then modified upon arrival to the Golgi complex producing the P2 form (69 kD), and finally processed to the mature form (67 kD) in the vacuole (Stevens et al., 1984). As shown in Fig. 8, wild-type strains and the *erv14Δ* strain exhibited similar kinetics for CPY transport to the vacuole, whereas the *sec12-4* temperature-sensitive mutation accumulated the ER form (P1) of CPY when shifted to a restrictive temperature. Similar results were observed for transport of the glycosylphosphatidylinositol-anchored plasma membrane protein Gas1p. Newly synthesized Gas1p appeared in the ER as a 105-kD glycosylphosphatidylinositol-anchored precursor that carries N- and O-linked oligosaccharide. As Gas1p traverses the Golgi complex, outer chain glycosylation residues are added, generating the 125-kD mature form (Nuoffer et al., 1991). Gas1p was transported out of the ER in wild-type and *erv14Δ* strains; however, we see a subtle delay in Gas1p transport (note the ratio of ER form to mature form after a 10-min pulse in the Gas1p panel in Fig. 8). This delay was not as severe as seen in strains bearing deletions of other Erv proteins, such as Emp24p and Erv25p (Belden and Barlowe, 1996). In *sec12-4* cells, the ER form of Gas1p accumulated but displayed a reduced electrophoretic mobility during the chase period, as has been previously observed (Schimmöller et al., 1995; Belden and Barlowe, 1996). Based on these results, we

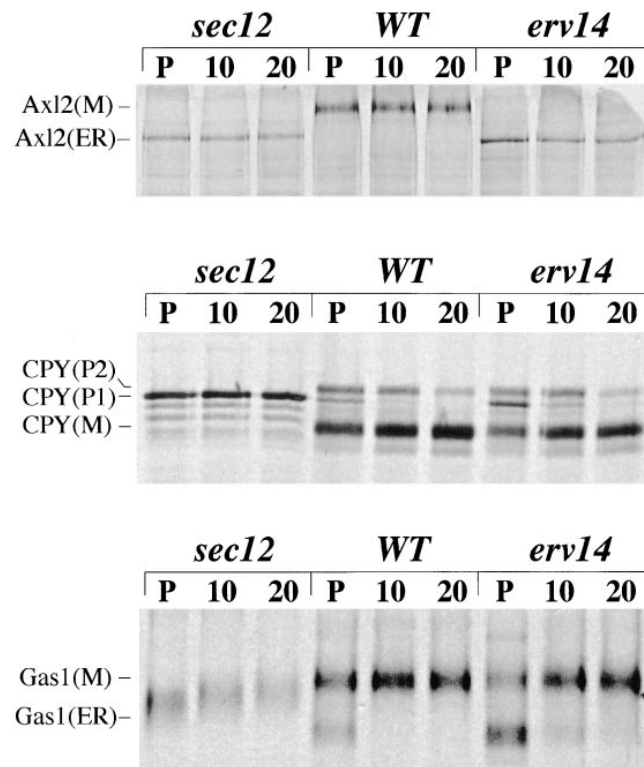


Figure 8. Pulse-chase analysis of secretory proteins in WT and *erv14Δ* strains. *sec12* strain CBY471, wild-type strain CBY461, and *erv14Δ* strain CBY463 were pulsed for 10 min followed by a chase of 10 and 20 min. Antibodies specific for Axl2p-HA, CPY, and Gas1p were used to immunoprecipitate labeled protein from a common extract. Immunoprecipitates were washed and resolved on 7.5 or 10% polyacrylamide gels, and labeled proteins were visualized by fluorography.

conclude that the *ERV14* gene is not required for transport of CPY and Gas1p from the ER to the Golgi complex, in contrast to *sec* mutant strains such as *sec12-4* (Novick et al., 1980; Stevens et al., 1984). This result is also consistent with the wild-type growth rate for *erv14Δ* since cell surface expansion (i.e., growth rate) was not impeded in these strains, again in contrast to typical *sec* mutations that are lethal and prevent expansion of the plasma membrane.

Transport of Axl2p was also examined in these strains. Strikingly, the transport block observed in an *erv14Δ* strain was as complete as seen in a *sec12-4* strain (Fig. 8). We could not detect the mature form of Axl2p in the *erv14Δ* strain even after the 20-min chase period. This result is consistent with the steady-state analysis in an *erv14Δ* strain conveyed though immunoblotting in Fig. 7, where the 150-kD form accumulated and the level of mature species was depleted. Furthermore, the 150-kD form of Axl2p that accumulated in an *erv14Δ* strain was relatively constant during the 20-min chase period, indicating that this species is not rapidly degraded. The transport of Axl2p from the ER to the Golgi appeared to occur rapidly. Several attempts were made to detect earlier secretory forms of Axl2p-3HA using shorter pulse time periods in larger-scale reactions, but we failed to detect ER and Golgi forms of this protein under these conditions. We speculate that a short transitory time coupled with the heterogeneity of modifications on Axl2p-3HA as it is transported through the secretory pathway prevents detection of these intermediates.

We proposed that Axl2p is not exported from the ER in *erv14Δ* strains and sought additional lines of evidence in support of this proposal. Axl2p acquires N-linked oligosaccharide in the ER of yeast cells (Roemer et al., 1996), and if the form that accumulates in an *erv14Δ* strain is trapped in the ER, treatment with Endo H should liberate this covalently linked carbohydrate and produce a faster migrating polypeptide on polyacrylamide gels (Orlean et al., 1991). After immunoprecipitation of Axl2p-3HA from various strains, treatment with Endo H produced an alteration in the mobility of the labeled polypeptide (Fig. 9). The forms of Axl2p-3HA that accumulated in an *erv14Δ* and a *sec12-4* strain displayed identical properties upon treatment with Endo H, shifting the ~150-kD ER-form to an ~125-kD species. Based on an approximation of each core oligosaccharide contributing 2 kD in mass (Orlean et al., 1991), we estimate the attachment of ~13 N-linked chains on Axl2p, which was predicted to contain 16 potential N-linked glycosylation sites (Roemer et al., 1996). Treatment of the mature form of Axl2p-3HA with Endo H also produced a distinct shift in size from ~220 to ~145 kD, but clearly not to the 125-kD species that appears after removal of N-linked residues from the ER form. We speculate that Axl2p acquires O-linked oligosaccharides in the ER that are then extended upon transport through the Golgi (Tanner and Lehle, 1987). Indeed, preliminary data indicate that Axl2p contains O-linked oligosaccharide (Sanders, S., and M. Gentsch, personal communication), which would also explain the difference between the predicted size (~90 kD) and the Endo H-treated ER form (~125 kD). Regardless, the form of Axl2p-3HA that accumulates in an *erv14Δ* strain behaves identically to the ER

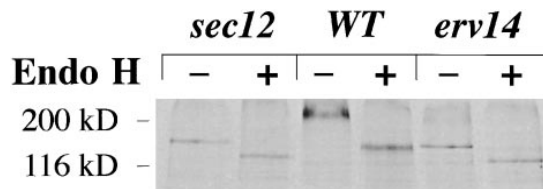


Figure 9. Endo H treatment of Axl2p. Immunoprecipitates of Axl2p-HA from *sec12* (CBY471), wild-type (CBY461), and *erv14Δ* (CBY463) were incubated in the absence (-) or presence (+) of Endo-H. Samples were resolved on a 7.5% polyacrylamide gel, and labeled species were visualized by fluorography.

form that accumulates in a *sec12-4* strain, a well-characterized mutant representative of mutants blocked in export from the ER (Novick et al., 1980; Stevens et al., 1984; Nakanishi et al., 1988). This observation, coupled with the fact that CPY and Gas1p are transported and modified correctly, make it unlikely that the *erv14Δ* mutation alters the glycosylation machinery producing modification defects on Axl2p.

As an independent method to evaluate Axl2p location in *erv14Δ* strains, we performed immunofluorescence experiments to visualize Axl2p-3HA in wild-type and *erv14Δ* strains. Axl2p is reported to localize to discrete sites at the cell periphery depending on the phase of the cell cycle and

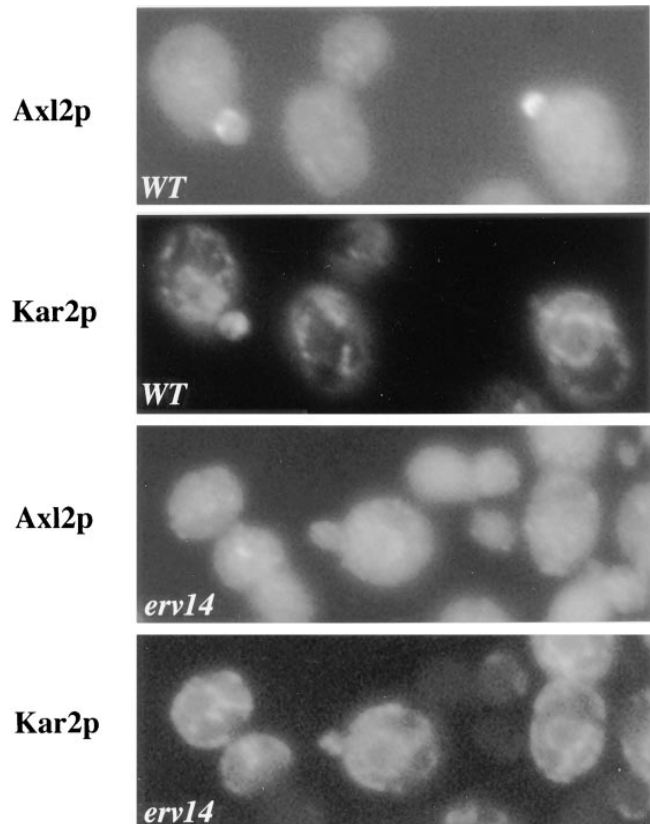


Figure 10. Axl2p is mislocalized in *erv14Δ* strains. Double-label immunofluorescence microscopy of wild-type (CBY461) and *erv14Δ* (CBY463) strains with Kar2p antiserum and anti-HA monoclonal antibody for Axl2p-HA detection. Note the distinct staining pattern for Axl2p-HA observed in wild-type cells that is absent in *erv14Δ* strains.

first appears in nascent buds as a crescent-shaped patch that then diffuses and appears as a ring at the mother-daughter bud neck (Roemer et al., 1996). Immunofluorescence images generated from double staining wild-type and *erv14Δ* strains with anti-HA and anti-Kar2p revealed the expected localization pattern for Axl2p-3HA in wild-type strains (Fig. 10). In contrast, we did not detect this staining pattern for Axl2p-3HA in *erv14Δ* strains after examination of several hundred stained cells. Axl2p-3HA appeared to colocalize with Kar2p in some images, but a definitive ER localization for Axl2p remained equivocal through this approach. The accumulation of Axl2p-3HA in the ER may produce a stain that is too diffuse for detection in this compartment. The validity of our immunofluorescence procedure for *erv14Δ* cells was confirmed by observation of a characteristic ER-staining pattern for Kar2p (Fig. 10). We can conclude that the normal localization pattern of Axl2p-3HA is blocked in an *erv14Δ* strain, and this result is entirely consistent with a block in export from the ER observed in the pulse-chase experiments.

Because immunofluorescence did not document the subcellular location of Axl2p-3HA in an *erv14Δ* strain, we performed cell fractionation experiments to determine where Axl2p accumulates in this strain. A standard magnesium-containing sucrose gradient method (Antebi and Fink, 1992) that resolves several yeast organelles was used to monitor the subcellular distribution of Axl2p in a wild-type and an *erv14Δ* strain. In a wild-type strain (Fig. 11, A and B), the mature form of Axl2p-3HA comigrates with the PMA and is resolved from Golgi (GDPase) and vacuolar (Vph1) membranes. The 150-kD form of Axl2p-3HA that accumulates in an *erv14Δ* strain (Fig. 11, C and D) comigrates with ER membranes (Sec61p) and is resolved

from Golgi and vacuolar membranes. However, the conditions of this gradient do not cleanly separate ER membranes (Sec61p) from plasma membranes (PMA), and we chose another sucrose gradient fractionation procedure to resolve these compartments. This method relies on a more vigorous lysis procedure in the presence of EDTA, a condition that strips ribosomes from the ER and produces a corresponding shift of ER membranes up in the gradient to a lower buoyant density (Kölling and Hollenberg, 1994; Roberg et al., 1997). As seen in Fig. 12, the 150-kD form of Axl2p-3HA observed in an *erv14Δ* strain coincides with the peak of Sec61p (Fig. 12, C and D) and is resolved from the PMA. Based on the fractionation patterns observed in Figs. 11 and 12, we conclude that Axl2p-3HA in *erv14Δ* strains is localized to the ER, a result that is entirely consistent with our pulse-chase and immunofluorescence experiments. Furthermore, these sucrose gradient analyses indicate that additional secretory proteins (PMA, GDPase, and Vph1) are synthesized and localized correctly in an *erv14Δ* strain.

Pleiotropic Effects of *erv14Δ* Mutations

To determine if *ERV14* deletion produced altered budding patterns in diploid cells, we constructed the homozygous disruptant strain CBY410. This diploid strain does not display a bud site selection defect (normal bipolar pattern), which is consistent with the observation that *axl2Δ* homozygous diploids are phenotypically bipolar (Roemer et al., 1996). However, we found that the homozygous *erv14Δ* disrupted strain would not sporulate under standard sporulation conditions (Sherman, 1991). We tested if *erv14Δ/erv14Δ* diploids became inviable under these con-

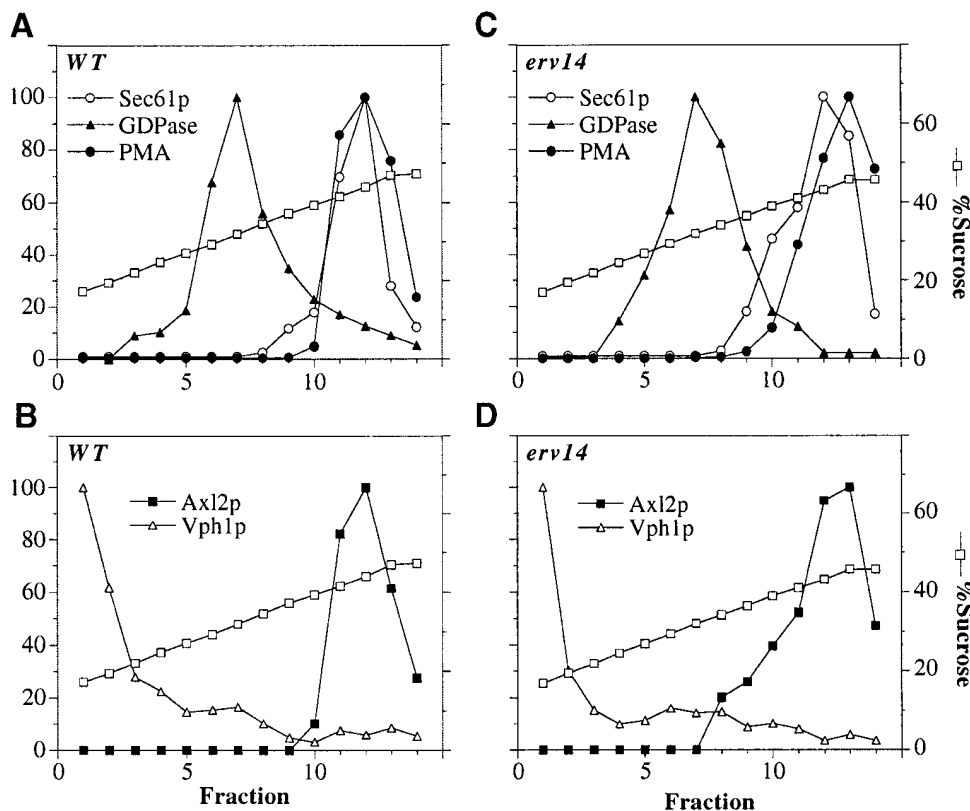


Figure 11. Sucrose gradient fractionation of Axl2p-3HA. Whole-cell lysates from wild-type strain CBY461 (A and B) and *erv14Δ* strain CBY463 (C and D) were separated on sucrose density gradients (20–60%) containing magnesium, and fractions were collected from the top. Relative levels of Sec61p (ER marker), PMA, Vph1 (vacuolar marker), and Axl2-3HA in each fraction were quantified by densitometry of immunoblots. GDPase (Golgi marker) was measured by enzymatic assay.

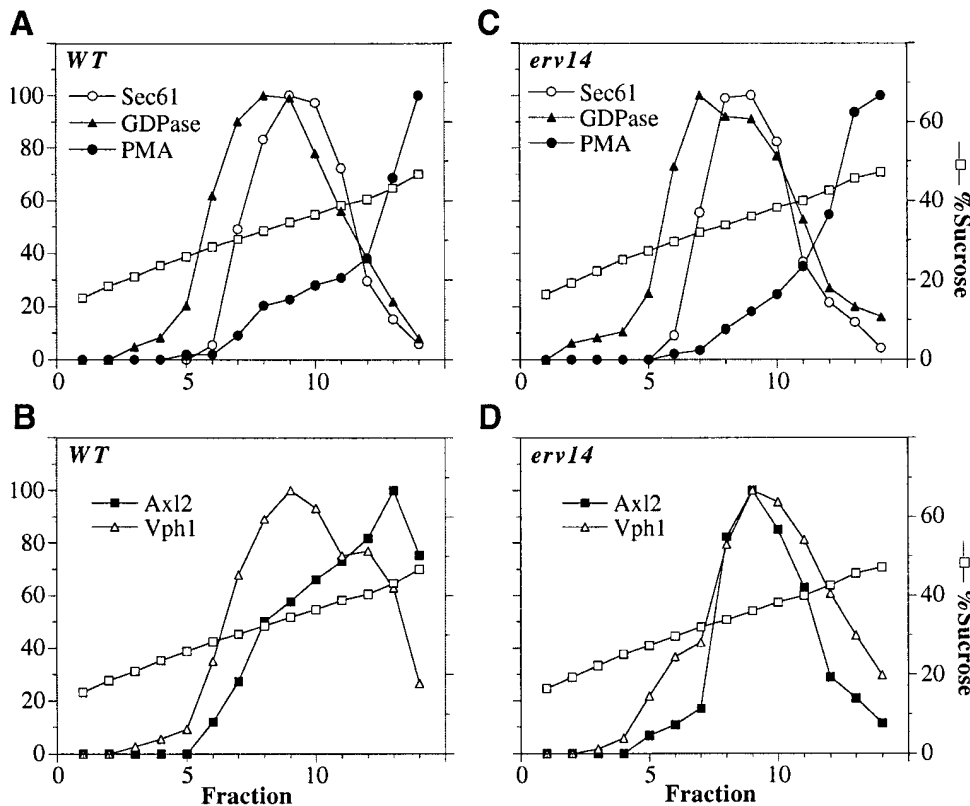


Figure 12. EDTA/sucrose gradient fractionation of Axl2p-3HA. Whole-cell lysates from wild-type strain CBY461 (A and B) and *erv14Δ* strain CBY463 (C and D) were separated on sucrose density gradients (20–60%) containing 10 mM EDTA, and fractions were collected from the top. Relative levels of Sec61p (ER marker), PMA, Vph1 (vacuolar marker), and Axl2-3HA in each fraction were quantified by densitometry of immunoblots. GDPase (Golgi marker) was measured by enzymatic assay.

ditions and found that the cell viability of wild-type (CBY453) and mutant (CBY410) cultures were similar after several days in sporulation media. Further, the mutant strains grew on nonfermentable carbon sources as efficiently as wild-type strains, indicating the carbon source contained in sporulation media is adequate. Finally, transformation of CBY410 with the *Erv14p*-HA plasmid (strain CBY433) restored sporulation competency to wild-type levels (Table III). These results indicate *Erv14p* is required for some aspect of sporulation.

Previous studies have shown that *Axl2p* is expressed at equal levels in both haploid and diploid cells, although this protein does not appear to participate in bud site selection in diploids (Roemer et al., 1996). We considered the possibility that delivery of *Axl2p* to the cell surface could also be required for efficient sporulation. Our previous results (Table II) demonstrated that overproduction of *Axl2p* partially suppressed the nonaxial budding phenotype of haploid *erv14Δ* strains. Therefore, we tested if overproduction of *Axl2p* could rescue the sporulation defect. However, the sporulation efficiency of homozygous *erv14Δ* dis-

ruptants was not affected by transformation with a multicopy version of *AXL2* (Table III). In summary, deletion of *ERV14* leads to defects in haploid bud site selection, in recovery from stationary phase growth and in sporulation of diploid cells. The nonaxial budding phenotype may be suppressed by overproduction of *Axl2p*, whereas recovery from stationary phase growth and sporulation were not affected by the expression level of *Axl2p*. These pleiotropic effects suggest *Erv14p* functions in other cellular processes besides transport of *Axl2p* and that perhaps gene products involved in sporulation rely on *Erv14p* for efficient transport.

Discussion

Organelles of the eukaryotic secretory pathway remain distinct in spite of dynamic anterograde and retrograde transport processes. Specific coat proteins that catalyze transport between the ER and Golgi are thought to contribute to this organization (Schekman and Orci, 1996), although the molecular mechanisms that link coat proteins with cellular sorting are not understood. Here we characterize a novel protein, termed *Erv14p*, that was discovered on ER-derived transport vesicles and appears to participate in sorting during ER to Golgi transport. *Erv14p* is an integral membrane protein that shares significant sequence identity (36%) and similarity (63%) over the entire length of the *Drosophila cornichon* gene product. Localization studies indicate that *Erv14p* resides in the ER and Golgi compartments of cells and is selectively packaged into ER-derived vesicles in a COPII-dependent manner. Disruption of the *ERV14* gene produces viable haploid cells that exhibit defects in axial bud site selection.

Table III. Sporulation of Diploid Cells

Strain	Number of tetrads	<i>n</i>
CBY453 (WT)	39	200
CBY410 (<i>erv14Δ/erv14Δ</i>)	0	200
CBY432 (<i>erv14Δ/erv14Δ</i> with <i>pRS316</i>)	0	200
CBY433 (<i>erv14Δ/erv14Δ</i> with <i>pRS-ERV14HA</i>)	34	200
CBY464 (<i>erv14Δ/erv14Δ</i> with <i>p2μm-AXL2</i>)	0	200

The results shown here are representative of three separate experiments. Sporulation was scored visually by looking for tetrads after 4 d in spmD medium. After 7 d, strains deficient for *ERV14* still had not sporulated.

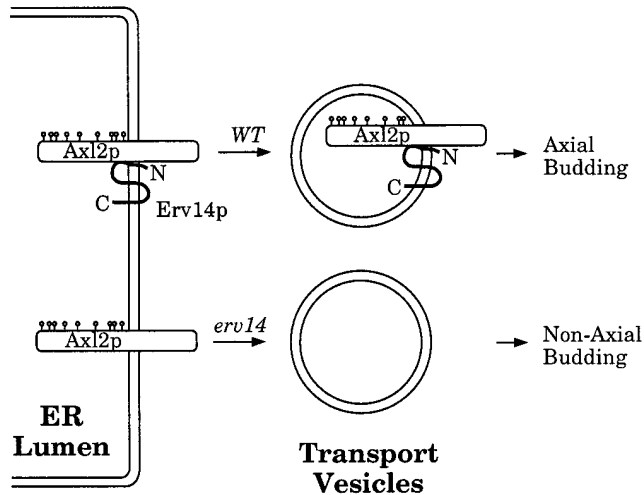


Figure 13. Model for Erv14p function in intracellular transport. In a wild-type strain (*WT*), Axl2p is efficiently packaged into ER-derived vesicles, and axial bud sites are established. In an *erv14Δ* strain, ER-derived vesicles are produced, but Axl2p fails to enter vesicles, and cells bud in a nonaxial manner.

This phenotype correlates with the failure of *erv14Δ* strains to transport a bud site selection protein (Axl2p) to the cell surface. We propose that Erv14p regulates export of Axl2p and possibly other secretory proteins from the ER in COPII-coated vesicles as depicted in Fig. 13.

Erv14p is composed largely of hydrophobic amino acids and possesses three linear segments of adequate hydrophobicity to span a lipid bilayer (Kyte and Doolittle, 1982). Application of the “positive inside” rule (von Heijne and Gavel, 1988) predicts a topology such that the NH₂ terminus is oriented toward the cytoplasm and the COOH terminus is oriented toward the luminal compartment. The first putative loop (amino acids 29–51) displays a net negative charge, whereas positively charged residues are enriched in loop two (amino acids 81–111). This charge distribution is highly conserved between Erv14p and *cornichon*, lending some credence to this topology prediction, but there are exceptions to the positive inside rule, and it is not possible to draw a firm conclusion about the transmembrane arrangement of Erv14p at this time. Because Erv14p is detected in the ER, ER-derived vesicles, and Golgi membranes, it appears that this molecule cycles between early compartments of the secretory pathway, and we speculate that amino acid residues in this protein impart selective packaging into COPII- and/or COPI-coated vesicles. Characterized sequence motifs proposed to mediate incorporation into COPII-coated vesicles (Nishimura and Balch, 1997; Dominguez et al., 1998) or COPI-coated vesicles (Nilsson et al., 1989; Cosson and Letourneur, 1994) are not found in Erv14p. Therefore, selective incorporation of Erv14p into ER-derived vesicles could be through direct interaction of COPII with novel signal(s) contained on the cytoplasmic surface(s) of Erv14p or through association of Erv14p with other proteins coupled to the COPII budding machinery.

Surprisingly, deletion of *ERV14* did not interfere with bulk secretory function but instead produced defects in yeast cell polarity. To comprehend this phenotype, we re-

viewed the literature concerning bud site selection in yeast. Haploid yeast cells exhibit an axial budding pattern whereby each new bud forms directly adjacent to the previous bud site. The selection of an appropriate bud site is thought to rely on a series of integrated events: first, the selected site for budding must be marked; second, components required for bud formation are assembled at this site; and third, the actin cytoskeleton and secretory apparatus are directed toward the selected site for growth of the emerging bud (Drubin, 1991). For the axial budding pattern, it has been proposed that this first stage is accomplished through a landmark that persists after cytokinesis and provides the cell with an assembly site for the next round of budding (Chant and Herskowitz, 1991; Snyder et al., 1991). Axl2p is unique among the characterized bud site selection proteins because it must be delivered to the plasma membrane via the secretory pathway. Once anchored in the plasma membrane, Axl2p may recruit additional components to the incipient bud site. In haploid *axl2Δ* strains, the axial budding pattern is lost, and a bipolar phenotype is observed such that ~50% of the newly formed buds are placed at the opposite pole from the previous bud site (Halme et al., 1996; Roemer et al., 1996).

When we examined *erv14Δ* strains, we observed a non-axial budding pattern and found that Axl2p accumulated in the ER. The accumulation of Axl2p in the ER provides a rational explanation for the nonaxial phenotype displayed by *erv14Δ* strains. Based on the following observations, however, we suspect that some Axl2p is slowly transported to the cell surface in *erv14Δ* strains. First, immunoblot analysis indicated that a low level of the mature form of Axl2p was detected in *erv14Δ* strains, although this species appears to be synthesized at a slow rate since it was not detected in pulse-chase experiments. Second, only ~16% of the *erv14Δ* cells exhibit budding from both poles in contrast to a more typical bipolar pattern observed in *axl2Δ* strains (Halme et al., 1996; Roemer et al., 1996). This may be explained if *erv14Δ* cells deliver some Axl2p to incipient bud sites, but with suboptimal levels of plasma membrane Axl2p, a nonaxial phenotype is displayed intermittently. Third, we find that overexpression of Axl2p partially suppressed the nonaxial budding phenotype in *erv14Δ* strains (Table II). Again, this observation may be explained if some Axl2p trickles through the secretory pathway in an *erv14Δ* strain, and overexpression of Axl2p increases the level of this flow.

Could the role of Erv14p in yeast trafficking provide insights on the function of *cornichon*? The *cornichon* mutants display phenotypes that are similar to *torpedo* (EGF receptor) and *gurken* (TGF α homologue and putative torpedo ligand) mutants. These three genes are components of an intercellular signaling process between germ-line cells and surrounding follicle cells that establishes anterior–posterior polarity during early stages of oogenesis. Both *gurken* and *cornichon* are required in germ-line cells, whereas *torpedo* function is required in surrounding follicle cells of the developing egg chamber. The localized delivery of *gurken* protein to the plasma membrane of the oocyte presumably activates the EGF receptor *torpedo* in a subset of follicle cells and specifies their posterior fate. In turn, the polarized arrangement of the surrounding follicle cells provides spatial information to the oocyte and is

critical for the reorganization of the microtubule network at mid-oogenesis. In *cornichon*, *gurken*, and *torpedo* mutants, intercellular signaling between the oocyte and surrounding follicle cells fails. Anterior markers are abnormally expressed in the posterior follicle cells, producing egg chambers that have the normal arrangement of oocyte and nurse cells but have duplicated anterior follicle cells at both poles. It is postulated that the *gurken* signal emanating from the oocyte represses anterior fates in adjacent follicle cells and directs them to a posterior fate (González-Reyes and St. Johnston, 1994; Roth et al., 1995). In *cornichon* mutants, *gurken* mRNA expression and perinuclear localization is normal. Examination of *gurken* protein reveals that the expression level is normal, but *cornichon* egg chambers display a diffuse staining pattern for *gurken* protein at the oocyte membrane, unlike the tight stripe-like distribution at the dorsal–anterior corner of the oocyte observed in wild-type. Indeed, one explanation offered for this phenotype was that an altered polarity in *cornichon* egg chambers would cause less efficient membrane targeting of vesicles transporting *gurken* protein (Roth et al., 1995).

In light of our findings with *erv14Δ* strains, it is plausible that in *cornichon* mutants, a landmark on the oocyte cell surface is not established to correctly orient the secretory pathway. Much as the yeast cell uses *Erv14p* to export *Axl2p* from the ER and mark the axial bud site, we speculate that *cornichon* is required for export of a polarity establishment factor from the oocyte ER in *Drosophila*. Although there are no candidates for this factor at present, the high degree of homology shared between *Erv14p* and the *cornichon* gene product suggests this molecule may be related to *Axl2p*.

The mechanism by which *Erv14p* catalyzes *Axl2p* export from the ER remains to be determined, and we can envision several possibilities to explain this transport block. First, *Erv14p* could directly bind to *Axl2p* and escort this protein out of the ER, acting as an adaptor for incorporation of *Axl2p* into COPII-coated vesicles. Direct binding could also be involved in the folding of *Axl2p* or assembly of *Axl2p* into an oligomeric complex before exit from the ER, although we do not favor this possibility because proteins involved in these processes (e.g., BiP) appear to remain in the ER and are not selectively packaged into ER-derived vesicles (Salama et al., 1993; Barlowe et al., 1994; Rexach et al., 1994). Furthermore, the forms of *Axl2p* that accumulate in the ER of *erv14Δ* and *sec12* strains are indistinguishable and are not rapidly degraded, suggesting that *Axl2p* is stably folded but unable to depart the ER. The *erv14Δ* phenotype resembles yeast strains that lack *Shr3p*, a resident ER protein that is required for the export of amino acid permease molecules in COPII-coated vesicles (Ljungdahl et al., 1992; Kuehn et al., 1996, 1998). However, the activities of *Erv14p* and *Shr3p* appear to be distinct because *Erv14p* is selectively packaged into COPII-coated vesicles, whereas *Shr3p* does not appear to enter these vesicles (Kuehn et al., 1996). Another set of ER proteins that produce selective transport defects (*Vma12p*, *Vma21p*, and *Vma22p*) are required for export of integral membrane subunits of the vacuolar ATPase (Hill and Stevens, 1994, 1995; Jackson and Stevens, 1997). It remains to be determined if these *Vma* proteins are se-

lected for incorporation into COPII-coated vesicles. However, it has been proposed that *Vma12p*, *Vma21p*, and *Vma22p* function in the assembly of V-ATPase subunits in the ER and that assembly is a prerequisite for export from the ER (Jackson and Stevens, 1997). At present, we are aware of only three proteins that when deleted produce selective ER to Golgi transport defects and are enriched on COPII-coated vesicles: *Emp24p* (Schimöller et al., 1995), *Erv25p* (Belden and Barlowe, 1996), and *Erv14p*. We continue to explore the protein–protein interactions and mechanisms by which these molecules influence sorting during transport from the ER.

We thank Bill Belden for help with strain construction, Terry Roemer and Michael Snyder for generously providing *AXL2* constructs, Hannele Ruohola and Trudi Schüpbach for helpful discussions on *Drosophila* development, and Sylvia Sanders for advice and sharing her unpublished observations.

This work was supported by grants from the National Institute of General Medical Sciences and the Pew Scholars Program in the Biomedical Sciences.

Received for publication 29 April 1998 and in revised form 9 July 1998.

References

- Antebi, A., and G.R. Fink. 1992. The yeast Ca^{2+} -ATPase homologue, *PMR1*, is required for normal Golgi function and localizes in a novel Golgi-like distribution. *Mol. Biol. Cell.* 3:633–654.
- Ashburner, M., P. Thomson, J. Roote, P.F. Lasko, Y. Grau, M. El Messal, S. Roth, and P. Simpson. 1990. The genetics of a small autosomal region of *Drosophila melanogaster* containing the structural gene for alcohol dehydrogenase. VII. Characterization of the region around the snail and cactus loci. *Genetics.* 126:679–694.
- Ausubel, R.M., R. Brent, R.E. Kingston, D.D. Moore, J.G. Seidman, J.A. Smith, and K. Struhl. 1987. Current Protocols in Molecular Biology. Greene Publishing Associates and Wiley-Interscience. 3.01–3.18.7.
- Baker, D., L. Hicke, M. Rexach, M. Schleyer, and R. Schekman. 1988. Reconstitution of SEC gene product-dependent intercompartmental protein transport. *Cell.* 54:335–344.
- Balch, W.E., J.M. McCaffery, H. Plutner, and M.G. Farquhar. 1994. Vesicular stomatitis virus glycoprotein is sorted and concentrated during export from the endoplasmic reticulum. *Cell.* 76:841–852.
- Barlowe, C., L. Orci, T. Yeung, M. Hosobuchi, S. Hamamoto, N. Salama, M. Rexach, M. Ravazzola, M. Amherdt, and R. Schekman. 1994. COPII: a membrane coat formed by Sec proteins that drive vesicle budding from the ER. *Cell.* 77:895–907.
- Baudin, A., O. Ozier-Kalogeropoulos, A. Denouel, F. Lacroute, and C.A. Cullin. 1993. A simple and efficient method for direct gene deletion in *Saccharomyces cerevisiae*. *Nucleic Acids Res.* 21:3329–3330.
- Bednarek, S.Y., M. Ravazzola, M. Hosobuchi, M. Amherdt, A. Perrelet, R. Schekman, and L. Orci. 1995. COPI- and COPII-coated vesicles bud directly from the endoplasmic reticulum in yeast. *Cell.* 83:1183–1196.
- Belden, W.J., and C. Barlowe. 1996. *Erv25p*, a component of COPII-coated vesicles, forms a complex with *Emp24p* that is required for efficient endoplasmic reticulum to Golgi transport. *J. Biol. Chem.* 271:26939–26946.
- Bender, A., and J.R. Pringle. 1989. Multicopy suppression of the *cdc24* budding defect in yeast by *CDC42* and three newly identified genes including the ras-related gene *RSR1*. *Proc. Natl. Acad. Sci. USA.* 86:9976–9980.
- Brodsky, J.L., and R. Schekman. 1993. A *Sec63p* complex from yeast is required for protein translocation in a reconstituted proteoliposome. *J. Cell Biol.* 123:1355–1363.
- Chant, J. 1996. Generation of cell polarity in yeast. *Curr. Opin. Cell Biol.* 8:557–565.
- Chant, J., and I. Herskowitz. 1991. Genetic control of bud site selection in yeast by a set of gene products that constitute a morphogenetic pathway. *Cell.* 65:1203–1212.
- Chant, J., and J.R. Pringle. 1995. Patterns of bud-site selection in the yeast *Saccharomyces cerevisiae*. *J. Cell Biol.* 129:751–765.
- Chant, J., K. Corrado, J.R. Pringle, and I. Herskowitz. 1991. Yeast *BUD5*, encoding a putative GDP-GTP exchange factor, is necessary for bud site selection and interacts with bud formation gene *BEM1*. *Cell.* 65:1213–1224.
- Chant, J., M. Mischke, E. Mitchell, I. Herskowitz, and J.R. Pringle. 1995. Role of *Bud3p* in producing the axial budding. *J. Cell Biol.* 129:767–778.
- Cosson, P., and F. Letourneur. 1994. Coatomer interaction with di-lysine endoplasmic reticulum retention motifs. *Science.* 263:1629–1631.
- d'Enfert, C., C. Barlowe, S. Nishikawa, A. Nakano, and R. Schekman. 1991. Structural and functional dissection of a membrane glycoprotein required for vesicle budding from the endoplasmic reticulum. *Mol. Cell. Biol.* 11:

- Dominguez, M., K. Dejeard, J. Fullekrug, S. Dahan, A. Fazel, J.P. Paccaud, D.Y. Thomas, J.J.M. Bergeron, and T. Nilsson. 1998. gp25L/emp24/p24 protein family members of the cis-Golgi network bind both COPI and II coatomer. *J. Cell Biol.* 140:751-765.
- Drubin, D. 1991. Development of cell polarity in budding yeast. *Cell.* 65:1093-1096.
- Feldmann, H., M. Aigle, G. Aljinovic, B. Andre, M.C. Baclet, C. Barthe, A. Baur, A.M. Becam, N. Biteau, E. Boles et al. 1994. Complete DNA sequence of yeast chromosome II. *EMBO (Eur. Mol. Biol. Organ.) J.* 13:5795-5809.
- Feuermann, M., J. de Montigny, S. Potier, and J.L. Souciet. 1997. The characterization of two new clusters of duplicated genes suggests a 'Lego' organization of the yeast *Saccharomyces cerevisiae* chromosomes. *Yeast.* 13:861-869.
- Frankhauser, C., and A. Conzelmann. 1991. Purification, biosynthesis and cellular localization of a major 125-kDa glycoposphatidylinositol-anchored membrane glycoprotein of *Saccharomyces cerevisiae*. *Eur. J. Biochem.* 195:439-448.
- Fugita, A., C. Oka, Y. Arikawa, T. Katagal, A. Tonouchi, S. Kuhara, and Y. Misumi. 1994. A yeast gene necessary for bud-site selection encodes a protein similar to insulin-degrading enzymes. *Nature.* 372:567-569.
- González-Reyes, A., and R.D. St. Johnston. 1994. Role of oocyte position in establishment of anterior-posterior polarity in *Drosophila*. *Science.* 266:639-642.
- Halme, A., M. Michelitch, E. Mitchell, and J. Chant. 1996. Bud10p resembles a transmembrane receptor and is part of the cell division remnant recognized for axial polarization and budding in yeast. *Curr. Biol.* 6:570-579.
- Hayashibe, M., and S. Katohda. 1973. Initiation of budding and chitin-ring. *J. Gen. Appl. Microbiol.* 19:23-39.
- Hicke, L., and R. Schekman. 1989. Yeast Sec23p acts in the cytoplasm to promote protein transport from the endoplasmic reticulum to the Golgi complex in vivo and in vitro. *EMBO (Eur. Mol. Biol. Organ.) J.* 8:1677-1684.
- Hill, K.J., and T.H. Stevens. 1994. Vma21p is a yeast membrane protein retained in the endoplasmic reticulum by a di-lysine motif and is required for the assembly of the vacuolar H⁺-ATPase complex. *Mol. Biol. Cell.* 5:1039-1050.
- Hill, K.J., and T.H. Stevens. 1995. Vma22p is a novel endoplasmic reticulum-associated protein required for assembly of the yeast vacuolar H⁺-ATPase complex. *J. Biol. Chem.* 270:22329-22336.
- Jackson, D.D., and T.H. Stevens. 1997. VMA12 encodes a yeast endoplasmic reticulum protein required for vacuolar H⁺-ATPase assembly. *J. Biol. Chem.* 272:25928-25934.
- Jones, J.S., and L. Prakash. 1990. Yeast *Saccharomyces cerevisiae* selectable markers in pUC18 polylinkers. *Yeast.* 6:363-366.
- Kaiser, C.A., R.E. Gimeno, and D.A. Shaywitz. 1997. Protein secretion, membrane biogenesis, and endocytosis. In *Yeast III*. Cold Spring Harbor Laboratory Press, Cold Spring Harbor, NY. 91-227.
- Kane, P.M., M.C. Kuehn, I. Howald-Stevenson, and T.H. Stevens. 1992. Assembly and targeting of peripheral and integral membrane subunits of the yeast vacuolar H⁺-ATPase. *J. Biol. Chem.* 267:447-454.
- Kölling, R., and C.P. Hollenberg. 1994. The ABC-transporter Ste6 accumulates in the plasma membrane in a ubiquitinated form in endocytosis mutants. *EMBO (Eur. Mol. Biol. Organ.) J.* 13:3261-3271.
- Kuehn, M.J., J.M. Hermann, and R. Schekman. 1998. COPII-cargo interactions direct protein sorting into ER-derived transport vesicles. *Nature.* 391:187-190.
- Kuehn, M.J., R. Schekman, and P.O. Ljungdahl. 1996. Amino acid permeases require COPII components and the ER resident membrane protein Shr3p for packaging into transport vesicles in vitro. *J. Cell Biol.* 135:585-595.
- Kyte, J., and R.F. Doolittle. 1982. A simple method for displaying the hydrophobic character of a protein. *J. Mol. Biol.* 157:105-132.
- Laemmli, U.K. 1970. Cleavage of structural proteins during the assembly of the head of bacteriophage T4. *Nature.* 227:680-685.
- Ljungdahl, P.O., C.J. Gimeno, C.A. Styles, and G.R. Fink. 1992. SHR3: a novel component of the secretory pathway specifically required for localization of amino acid permeases in yeast. *Cell.* 71:463-478.
- Nakano, A., D. Brada, and R. Schekman. 1988. A membrane glycoprotein, Sec12p, required for transport from the endoplasmic reticulum to the Golgi apparatus in yeast. *J. Cell Biol.* 107:851-863.
- Nilsson, B., and L. Abrahamsen. 1990. Fusions to staphylococcal protein A. *Methods Enzymol.* 185:144-161.
- Nilsson, T., M. Jackson, and P.A. Peterson. 1989. Short cytoplasmic sequences serve as retention signals for transmembrane proteins in the endoplasmic reticulum. *Cell.* 58:707-718.
- Nishimura, N., and W.E. Balch. 1997. A di-acidic signal required for selective export from the endoplasmic reticulum. *Science.* 277:556-558.
- Novick, P., C. Field, and R. Schekman. 1980. Identification of 23 complementation groups required for post-translational events in the yeast secretory pathway. *Cell.* 21:205-215.
- Nuoffer, C., P. Jenö, A. Conzelmann, and H. Riezman. 1991. Determinants for glycopospholipid anchoring of the *Saccharomyces cerevisiae* GAS1 protein to the plasma membrane. *Mol. Cell Biol.* 11:27-37.
- Orlean, P., M.J. Kuranda, and D.F. Albright. 1991. Analysis of glycoproteins from *Saccharomyces cerevisiae*. *Methods Enzymol.* 194:682-697.
- Pringle, J.R. 1991. Staining of bud scars and other cell wall chitin with calcofluor. *Methods Enzymol.* 194:732-734.
- Pringle, J.R., A.E.M. Adams, D.G. Drubin, and B.K. Haarer. 1991. Immunofluorescence method for yeast. *Methods Enzymol.* 194:565-601.
- Quinn, P., G. Griffiths, and G. Warren. 1984. Density of newly synthesized plasma membrane proteins in intracellular membranes II. *Biochemical studies. J. Cell Biol.* 98:2142-2147.
- Rexach, M.F., M. Latterich, and R.W. Schekman. 1994. Characteristics of endoplasmic reticulum-derived transport vesicles. *J. Cell Biol.* 126:1133-1148.
- Roberg, K.J., N. Rowley, and C.A. Kaiser. 1997. Physiological regulation of membrane protein sorting late in the secretory pathway of *Saccharomyces cerevisiae*. *J. Cell Biol.* 137:1469-1482.
- Roemer, T., D. Madden, J. Chang, and M. Snyder. 1996. Selection of axial growth sites in yeast requires Axl2p, a novel plasma membrane glycoprotein. *Genes Dev.* 10:777-793.
- Rose, M.D., L.M. Misra, and J.P. Vogel. 1989. KAR2, a karyogamy gene, is the yeast homologue of the mammalian BiP/GRP78 gene. *Cell.* 57:1211-1221.
- Roth, S., R.S. Neuman-Silberberg, G. Barcelo, and T. Schüpbach. 1995. Cornichon and the EGF receptor signaling process are necessary for both anterior-posterior and dorsal-ventral pattern formation in *Drosophila*. *Cell.* 81:967-978.
- Rothblatt, J.A., R.J. Deshaies, S.L. Sanders, G. Daum, and R. Schekman. 1989. Multiple genes are required for proper insertion of secretory proteins into the endoplasmic reticulum in yeast. *J. Cell Biol.* 109:2641-2652.
- Salama, N.R., T. Yeung, and R. Schekman. 1993. The Sec13p complex and reconstitution of vesicle budding from the ER with purified cytosolic proteins. *EMBO (Eur. Mol. Biol. Organ.) J.* 12:4073-4082.
- Sanders, S.L., and I. Herskowitz. 1996. The Bud4 protein of yeast, required for axial budding, is localized to the mother/bud neck in a cell cycle-dependent manner. *J. Cell Biol.* 134:413-427.
- Sato, M., K. Sato, and A. Nakano. 1996. Endoplasmic reticulum localization of Sec12p is achieved by two mechanisms: Rer1p-dependent retrieval that requires the transmembrane domain and Rer1p-independent retention that involves the cytoplasmic domain. *J. Cell Biol.* 134:279-293.
- Schekman, R., and L. Orci. 1996. Coat proteins and vesicle budding. *Science.* 271:1526-1533.
- Schimmöller, F., B. Singer-Krüger, S. Schröder, U. Krüger, C. Barlowe, and H. Riezman. 1995. The absence of Emp24p, a component of ER-derived COPII-coated vesicles, causes a defect in transport of selected proteins to the Golgi. *EMBO (Eur. Mol. Biol. Organ.) J.* 14:1329-1339.
- Schröder, S., F. Schimmöller, B. Singer-Krüger, and H. Riezman. 1995. The Golgi-localization of yeast Emp47p depends on its di-lysine motif but is not affected by the ret1-1 mutation in α -COP. *J. Cell Biol.* 131:895-912.
- Sherman, F. 1991. Getting started with yeast. *Methods Enzymol.* 194:3-20.
- Sikorski, R.S., and P. Hieter. 1989. A system of shuttle vectors and yeast host strains designed for efficient manipulation of DNA in *Saccharomyces cerevisiae*. *Genetics.* 122:19-27.
- Snyder, M., S. Gehrung, and B.D. Page. 1991. Studies concerning the temporal and genetic control of cell polarity in *Saccharomyces cerevisiae*. *J. Cell Biol.* 114:515-532.
- Stevens, T., B. Esmon, and R. Schekman. 1984. Early stages in the yeast secretory pathway are required for transport of carboxy peptidase Y to the vacuole. *Cell.* 30:439-448.
- Stirling, C.J., J. Rothblatt, M. Hosobuchi, R. Deshaies, and R. Schekman. 1992. Protein translocation mutants defective in the insertion of integral membrane proteins into the endoplasmic reticulum. *Mol. Biol. Cell.* 3:129-142.
- Tanner, W., and L. Lehle. 1987. Protein glycosylation in yeast. *Biochim. Biophys. Acta.* 906:81-99.
- Towbin, H., T. Staehelin, and J. Gordon. 1979. Electrophoretic transfer of proteins from polyacrylamide gels to nitrocellulose sheets: procedure and some applications. *Proc. Natl. Acad. Sci. USA.* 76:4350-4354.
- von Heijne, G., and Y. Gavel. 1988. Topogenic signals in integral membrane proteins. *Eur. J. Biochem.* 174:671-678.
- Wilson, I.A., H.L. Niman, R.A. Houghton, A.R. Cherenon, M.L. Connolly, and R.A. Lerner. 1984. The structure of an antigenic determinant in a protein. *Cell.* 37:767-778.
- Winston, F., C. Dollard, and L.L. Ricupero-Hovasse. 1995. Construction of a set of convenient *Saccharomyces cerevisiae* strains that are isogenic to S288C. *Yeast.* 11:53-55.
- Woodcock, D.M., P.J. Crowther, J. Doherty, S. Jefferson, E. DeCruz, M. Noyer-Weidner, S.S. Smith, M.Z. Michael, and M.W. Graham. 1989. Quantitative evaluation of *Escherichia coli* host strains for tolerance to cytosine methylation in plasmid and phage recombinants. *Nucleic Acids Res.* 17:3469-3478.
- Yanagisawa, K., D. Resnick, C. Abeijon, P.W. Robbins, and C.B. Hirschberg. 1990. A guanidine diphosphatase enriched in Golgi vesicles of *Saccharomyces cerevisiae*: purification and characterization. *J. Biol. Chem.* 265:19351-19355.
- Yeung, T., C. Barlowe, and R. Schekman. 1995. Uncoupled packaging of targeting and cargo molecules during transport vesicle budding from the endoplasmic reticulum. *J. Biol. Chem.* 270:30567-30570.